Proceedings of the International Congress on Advances in Applied Physics and Materials Science, Antalya 2011

Effects of SiC Particle Size on Properties of Cu–SiC Metal Matrix Composites

G. Celebi Efe*, I. Altinsoy, M. Ipek, S. Zeytin and C. Bindal

Engineering Faculty, Department of Metallurgy and Materials Engineering, Sakarya University

Esentepe Campus, 54187 Sakarya, Turkey

This paper was focused on the effects of particle size and distribution on some properties of the SiC particle reinforced Cu composites. Copper powder produced by cementation method was reinforced with SiC particles having 1 and 30 μm particle size and sintered at 700 °C. Scanning electron microscopy studies showed that SiC particles were dispersed in copper matrix homogeneously. The presence of Cu and SiC components in composites were verified by X-ray diffraction analysis technique. The relative densities of Cu–SiC composites determined by Archimedes' principle are ranged from 96.2% to 90.9% for SiC with 1 μm particle size, 97.0% to 95.0% for SiC with 30 μm particle size. Measured hardness of sintered compacts varied from 130 to 155 HVN for SiC having 1 μm particle size, 188 to 229 HVN for SiC having 30 μm particle size. Maximum electrical conductivity of test materials was obtained as 80.0% IACS (international annealed copper standard) for SiC with 1 μm particle size and 83.0% IACS for SiC with 30 μm particle size.

PACS: 81.05.Ni, 81.20.Ev

1. Introduction

Copper, possessing a desirable combination of physical properties, have been utilized in quite a variety of applications since antiquity [1]. In terms of electrical behavior copper has the second highest electrical conductivity of any element just after silver [2]. Due to the high electrical and thermal conductivity, good corrosion resistance and high melting point, copper and copper based materials are widely used in thermal and electronic applications, i.e. electronic packaging, electrical contacts and resistance welding electrodes. Nevertheless, the low mechanical property at both room and high temperatures limits the extensive application of pure copper [3, 4].

The incorporation of ceramic particulate reinforcement can improve the high temperature mechanical property and wear resistance significantly, without severe deterioration of thermal and electrical conductivity of the matrix. Therefore, these kinds of materials are considered to be promising candidates for applications where high conductivity, high mechanical property and good wear resistance are required [4].

SiC could be used as a reinforcement to enhance the copper matrix. SiC/copper composites combine both the superior ductility and toughness of copper and the high strength and high modulus of SiC reinforcements [5].

In this study copper powder was produced by cementation method. Cementation is a general term used in the hydrometallurgical industry for the recovery of any dissolved metal from aqueous solution by contact reduction. More precisely, cementation, or displacement is described as the electrochemical precipitation of a metal from solution by another more electropositive metal [6]. This technique is a type of corrosion reaction in which the anodic half reaction is the dissolution of the less noble metal and the cathodic half reaction is the deposition of the more noble metal.

The present study concerns the copper–iron system and the corresponding global cementation reaction is $Cu^{2+} + Fe \rightarrow Cu^{+}Fe^{2+}$ [7]. At the present study cemented Cu matrix–SiC composites were produced by powder metallurgy method and the influence of the concentration and particle size of SiC on mechanical and electrical properties of composites were studied. The original aspect of present study is to produce cemented Cu matrix–SiC composites by powder metallurgy method on which very few works are available in the open literature.

2. Experimental procedure

Copper powder was produced by cementation method. Cementation of copper was performed by precipitating from $CuSO_4$ solutions using metallic iron powder.

Fig. 1. Schematic illustration of copper powder produced by cementation method.

The cementation process was illustrated in Fig. 1. The copper sulfate salt was dissolved in distilled water to produce a 0.1 M solution. The pH was adjusted to 2 by adding H_2SO_4 into the solution and the solution was stirred continuously for 20 min with adding stoichiometric ratio of Fe powder. Following to precipitation process, solution was cleaned with solution in a pH of 2 for twice, and then washed with distilled water for twice. After that, copper slurry was dried in a vacuum oven at

* corresponding author; e-mail: gcelebi@sakarya.edu.tr

80 °C for 2 h and copper powder was obtained. SiC particles were mixed mechanically with the calculated amount of cemented copper powder and were pressed in a steel mold of 15 mm in diameter with an axial pressure of 280 MPa and sintered at 700 °C in an open atmospheric furnace for 2 h embedded in graphite. Following sintering, compacts were immediately pressed with a load of 850 MPa, while sintered compacts were still hot, to have higher relative density and electrical conductivity. The microstructures of specimens were examined by scanning electron microscopy (SEM). In order to detect the Cu, SiC and any oxide of Cu and SiC particles X-ray diffraction (XRD) and energy dispersive spectroscopy (EDS) analyses were performed. Relative densities of cemented copper and Cu–SiC composites were determined according to Archimedes' method. Microhardness of both pure copper and composites were determined using a Leica WMHT-Mod model Vickers hardness instrument under an applied load of 50 g for 1 μm particle sized SiC and 100 g for 30 μm particle sized SiC. The measurements of electrical conductivity of specimens were performed on a GE model electric resistivity measurement instrument.

3. Results and discussion

Sintered pure copper sample was etched by 40%HNO_3–H_2O solution to see the grain structure. It is seen from Fig. 2a that the morphology of cemented Cu grains are approximately spherical shape and significant agglomeration which was observed in the Cu grains, even as the size of these agglomerations is between 2 and 6 μm. Fe, oxygen and S were detected in the EDS analyses probably as a result from the production of Cu powders by cementation process. SEM micrograph of sintered Cu–2 wt%SiC composite having 1 μm particle sized SiC was given in Fig. 2b at the same magnification of Fig. 2a for seeing where the SiC particles were located in. In micrographs Cu matrix seems as light grey and SiC particles seem as dark grey. SiC particles are dispersed in Cu matrix homogeneously and generally located in grain boundaries.

SEM microstructures with SEM-EDS surface analysis of Cu–5 wt%SiC composites with 1 μm and 30 μm particle sized SiC are shown in Fig. 3a,b. SiC particles in 1 μm particle size were distributed homogeneously in the copper matrix. In Cu–SiC composites reinforced with 30 μm particle sized SiC, free copper regions are in a majority due to the grain size of SiC and there is a good bonding between copper matrix and SiC particles. Probably for this reason oxygen contents in the surface maps decreased with increasing particle size of SiC. In Fig. 3b iron rich areas seem as light grey and it probably results from cementation process and oxidation at sintering temperature.

SEM map analysis of Cu–3 wt%SiC with 1 μm particle size shows that black shapes indicate SiC particles and oxygen and aluminium exist together and areas including iron contain oxygen at the same ratio (Fig. 4).

Element, wt%	Marks			
	1	2	3	4
O	35.0	33.7	30.4	
S	2.7	2.41		
Fe	35.8	25.3	26.7	
Cu	26.3	38.5	42.7	100

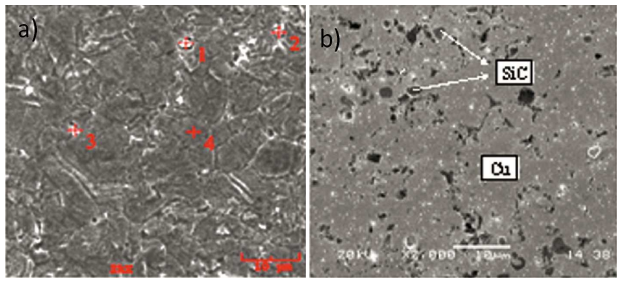

Fig. 2. (a) SEM-EDS analysis of sintered and etched pure copper, (b) SEM micrograph of sintered Cu–2 wt%SiC composite having 1 μm particle sized SiC.

a)	wt%		b)	wt%
O	7.67		C	8.26
Al	0.43		O	2.06
Si	13.1		Al	0.20
Fe	1.41		Si	25.5
Cu	77.2		Fe	0.51
			Cu	63.3

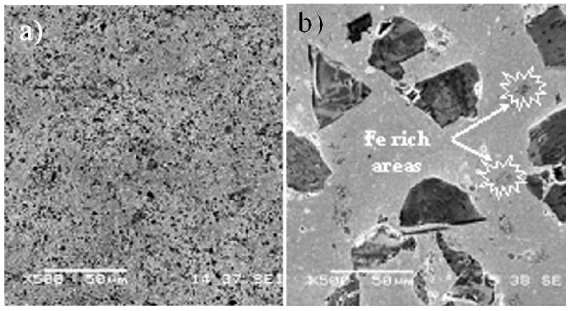

Fig. 3. SEM micrographs and EDS analysis of sintered (a) Cu–5 wt%SiC composite with 1 μm particle sized SiC, (b) Cu–5 wt%SiC with 30 μm particle sized SiC.

Figure 5 shows XRD diffraction patterns of the composites. It was found that the dominant components are copper and SiC. In Fig. 5a slight amount of iron oxide (Fe_3O_4) was detected probably resulting from the cementation process of copper powder.

Relative density, hardness and electrical conductivities of composites were given in Table. The density and electrical conductivity increased with increasing the size of SiC but decreased with increasing weight percentage of SiC. In composite with low SiC volume fraction, smaller Cu–SiC interface means smaller copper atom diffusion barrier, copper atoms can diffuse easily and fill

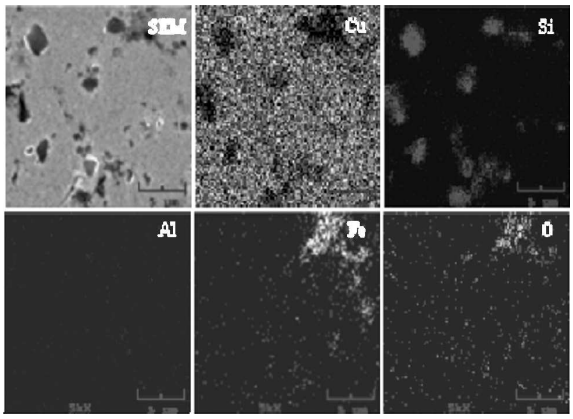

Fig. 4. EDS map analysis of sintered Cu–3 wt%SiC composite with 1 μm particle sized SiC.

the interstices between the SiC particles, thus leading to a higher densification of the composite [8, 9]. Also due to the lower relative density of SiC than copper, relative density of composite decreases with increasing amount of SiC.

As it is well known, the hardness of ductile copper can be improved by dispersion of second hard phase [10] and it is seen from Table that hardness of composites increased with both weight percentage and particle size of SiC. SiC particles adding into the pure copper increases the electrical resistivity via distorting the structure and so electrical conductivity of composites decreases with increase of the amount of SiC. The results indicate that Cu–SiC composite with 30 μm particle sized SiC has superior properties than the Cu–SiC composite with 1 μm particle sized SiC.

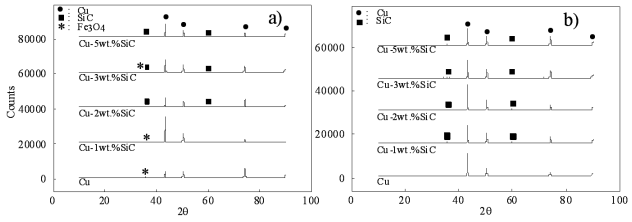

Fig. 5. XRD analysis of cemented Cu and Cu–SiC composites: (a) with 1 μm SiC and (b) with 30 μm SiC sintered at 700 °C for 2 h.

TABLE

Relative density, hardness and electrical conductivity values of Cu and Cu–SiC composites.

wt% SiC	Relative density [%]		Hardness [HV]		% IACS	
	1 μm SiC	30 μm SiC	1 μm SiC	30 μm SiC	1 μm SiC	30 μm SiC
0	97.5 ± 0.8	97.5 ± 0.8	127 ± 1.2	127 ± 1.2	91.7 ± 1.8	91.7 ± 1.7
1	96.2 ± 1.3	97.0 ± 1.3	130 ± 2.8	188 ± 13.8	79.0 ± 1.4	83.0 ± 0.7
2	95.5 ± 1.7	96.5 ± 0.4	139 ± 7.6	192 ± 14.0	72.8 ± 1.0	80.5 ± 1.4
3	92.3 ± 1.1	95.4 ± 0.3	142 ± 6.0	202 ± 15.0	66.4 ± 0.9	72.4 ± 1.5
5	90.9 ± 1.2	95.0 ± 1.1	155 ± 0.6	229 ± 30.0	54.9 ± 1.2	69.0 ± 1.8

Acknowledgments

The authors thank to expert Fuat Kayis for performing XRD and SEM-EDS studies and special appreciations are extended to technician Ersan Demir of Sakarya University for assisting with experimental studies. This work was conducted as project supported by TUBITAK with contract number of 106M118.

References

[1] W.D. Callister, D.G. Rethwisch, *Fundamentals of Materials Science and Engineering*, Wiley, 2008.

[2] `http://en.wikipedia.org/wiki/Copper` .

[3] R. Zhang, L. Gao, J. Guo, *Ceram. Int.* **30**, 401 (2004).

[4] Y. Zhan, G. Zhang, *Mater. Lett.* **57**, 4583 (2003).

[5] G.Ç. Efe, I. Altınsoy, T. Yener, M. Ipek, S. Zeytin, C. Bindal, in: *4th Int. Conf. on Powder Metallurgy, Craiova (Romania)*, Eds. H. Danninger, M. Mangra, I. Vida-Sim, Craiova 2009.

[6] B. Hiskey, J. Lee, *Hydrometallurgy* **69**, 45 (2003).

[7] W. Djoudi, F. Aissani, S. Bourouina, *Chem. Eng. J.* **133**, 1 (2007).

[8] J. Zhu, L. Liu, H. Zhao, B. Shen, W. Hu, *Mater. Des.* **28**, 1958 (2007).

[9] G.Ç. Efe, I. Altinsoy, M. Ipek, S. Zeytin, C. Bindal, *Kovove Materialy-Metal. Mater.* **49**, 131 (2011).

[10] G. Celebi Efe, I. Altinsoy, T. Yener, M. Ipek, S. Zeytin, C. Bindal, *Vacuum* **85**, 643 (2010).